LANGMUIR

Article

Ratiometric sensing of polycyclic aromatic hydrocarbons using capturing ligands functionalized mesoporous Au nanoparticles as surface-enhanced Raman scattering substrate

Dongjie Zhang, Rui Hao, Lingling Zhang, Hongjun You, and Jixiang Fang

Langmuir, **Just Accepted Manuscript** • DOI: 10.1021/acs.langmuir.0c02271 • Publication Date (Web): 02 Sep 2020

Ratiometric sensing of polycyclic aromatic hydrocarbons using capturing ligands functionalized mesoporous Au nanoparticles as surface-enhanced Raman scattering substrate

Dongjie Zhang[1], Rui Hao[1], Lingling Zhang[1], Hongjun You[2], Jixiang Fang[1]*

[1]*Key Laboratory for Physical Electronics and Devices of the Ministry of Education, School of Electronic Science and Engineering, Faculty of Electronic and Information Engineering, Xi'an Jiaotong University, Xi'an, Shann xi, 710049, China*

[2.] *School of Science, Xi'an Jiaotong University, Xi'an, Shann xi, 710049, China*

ABSTRACT:

The absorption behavior between plasmonic nanostructures and target molecule play key roles in an effective SERS detection. However, for analytes with low surface affinity to the metallic surface, e.g., polycyclic aromatic hydrocarbons (PAHs), it remains challenges to observe enhanced Raman signal. In this work, we reported a ratiometric SERS strategy for sensitive PAHs detection through the surface functionalization of 3D ordered mesoporous Au nanoparticles (*meso*-Au NPs). By employing mono-6-thio-β-cyclodextrin (HS-β-CD) as capture ligands, the hydrophobic molecules, e.g., anthracene, could be effectively absorbed on the *meso*-Au NPs surface via a host–guest interaction. Besides, a hydrophobic slippery surface is used as a concentrator to deliver and enrich the Au/analyte suspensions into a small sized area. Consequently, the detection limits of anthracene and naphthalene are down to 1 ppb and 10 ppb. The improved SERS enhancement is mainly ascribed to the host-guest effect of HS-β-CD ligands, large surface area and high-density of sub-10 nm mesopores of Au networks, as well as the enrichment effect of hydrophobic slippery surface. Moreover, the HS-β-CD (480 cm^{-1} band) could serve as an internal standard, leading to the ratiometric determination of anthracene ranging from 1 ppm to 1 ppb. The proposed surface modification strategy in combination with hydrophobic slippery surface shows great potential for active capture and trace detection of persistent organic pollutants in real-world SERS applications.

* To whom correspondence should be addressed. E-mail: jxfang@mail.xjtu.edu.cn.

INTRODUCTION

Being one of the most powerful vibrational spectroscopy techniques, surface-enhanced Raman scattering (SERS) has been applied in various fields, e.g., electrochemistry, catalysis, biosensing, food safety and environmental monitoring.[1-8] Metallic colloids i.e. Au or Ag NPs, are widely used as SERS-active substrates, due to their ease of synthesis, low-cost, commercial availability and remarkable Raman enhancement.[9-15] As a relatively complicated system, SERS detection refers to the interactions among incident light, plasmonic nanostructures, and probe molecules. The Raman signal is generally improved by either increasing the plasmonic activity of SERS substrate or by enhancing the interaction between the analytes and the substrate.[16-18] In addition to the fabrication of optimized SERS substrates with high density of "hot spots", it is also very important to enhance the ability of plasmonic nanostructures to effectively capture the target molecules.[19-23] SERS enhancement is surface dependent, and the Raman signal will only undergo enhancement when the analyte is physically or chemically adsorbed to the SERS-active metallic surface where the large electromagnetic field is localized.[24-28] In general, only the target analytes that have a strong affinity toward the metallic SERS-active surface can yield strong Raman signals. For molecules with a small surface affinity or weak Raman activity, it remains challenges to observe enhanced SERS signal.

Polycyclic aromatic hydrocarbons (PAHs), a kind of ubiquitous persistent organic pollutants (POPs), have attracted worldwide attention because of their strong carcinogenic, mutagenic and biological accumulation properties.[29-31] Owing to the apolar aromatic rings structure, most PAHs molecules show a very low affinity to a metallic surfaces and exhibit no resonance Raman scattering with visible-near-infrared excitation, which prevents their efficient SERS detection. To tackle this challenge, great efforts have been devoted to realizing the surface functionalization of plasmonic nanostructures, which would promote the binding of target analytes to the SERS-active surface.[32-34] Supramolecular host molecules e.g., crown ethers, resorcinarenes, calixarenes, and cyclodextrins, have received huge attentions for their sensitive identification and detection of organic compounds, especially water-insoluble analytes.[35-40] It was reported that mono-6-thio-β-cyclodextrin (HS-β-CD) could be modified onto the metal surface because of the host-guest interactions. PAHs molecule preferred to

enter the hydrophobic cavity and then forms an inclusion complex with β-CD, leading to enhanced Raman signals.[35,39] However, the sensitivity and reliability properties of SERS detection still remain a persistent issue, although the Raman signals of PAHs could be enhanced via the surface modifications of colloidal Au or Ag NPs. The irreproducible Raman signals arising from the uneven distributions of "hot spots", may significantly influences the practical applications.

Here, we reported an efficient and sensitive SERS method for PAHs determination based on the capturing ligands modified *meso*-Au NPs, which was prepared by a soft-enveloping strategy in our previous report.[41] HS-β-CD, one of the typical cyclodextrin molecules, was employed to attract PAHs analytes close to the designed SERS-active metallic surface via a host-guest interaction. Compared to other PAHs detection approaches based on the surface functionalization, our SERS strategy has multiple merits for chemical sensing, including: (i) an improved absorption and modification performance due to the features of large surface area and high-density mesopores for Au networks; (ii) the sensitive SERS signals enhanced by the *meso*-Au NPs with interconnected porous configuration; (iii) the enrichment effect of Au/analytes complexes based on the hydrophobic slippery surface. In this study, anthracene and naphthalene were employed as the probe molecules and the lowest detection concentrations could be down to 1 ppb and 10 ppb respectively. Moreover, HS-β-CD molecule with a specific vibrational signature would provide an internal standard to improve the reliability of PAHs sensing, showing huge potential for practical quantitative SERS applications.

EXPERIMENTAL SECTION

Materials. KIT-6 template was purchased from Nanjing Xianfeng Tech Co., Ltd.; $HAuCl_4 \cdot 4H_2O$, 1,1,3,3-tetramethyldisiloxane (TMDS), PVP (1×10^4 g·mol^{-1}), hydrofluoric acid (HF, 40%), mono-6-thio-β-cyclodextrin (HS-β-CD), tolune, hexane, sodium borohydride ($NaBH_4$) and ethanol were purchased from Sigma Aldrich Tech Co., Ltd.; Hydrophobic Teflon membrane (0.1 μm of pore size) was purchased from Whatman Corporation; Perfluorinated fluids (Krytox, GPL 105) were purchased from Dupont Corporation; Anthracene and naphthalene molecules were received from Aladdin Corporation. All

chemicals were used without further purification. Water used throughout the synthesis was Ultrapure DI (18.2 MΩ, Millipore).

Synthesis of the ordered *meso*-Au NPs. The mesoporous Au NPs were prepared by a soft-enveloping strategy. In brief, A solution of $HAuCl_4$·in ethanol (0.5 mL, 0.1 M) was added to the KIT-6 powder (10 mg), and then dried under reduced vacuum in order to incorporate the Au precursor into the mesoporous template. After the complete drying, the yellow-colored powder was dispersed in 0.3 mL of hexane. Then, 50 μL of TMDS was added to the hexane solutions. The Au deposition reaction was carried out in a closed vessel for 12 h, while the mixture color was changed from yellow to black. In order to obtain mesoporous Au NPs with excellent dispersity and stability, a multi-step procedure should be carried out, including template removal, ligands modification and surface purification. Firstly, toluene was used to remove the residual TMDS ligands before the KIT-6 removal. Then, the ordered Au networks/silica mixture was modified with PVP capping agent to avoid the aggregation of Au NPs. Lastly, a diluted HF solution was employed to etch the silica template, and 10 mM of $NaBH_4$ solution was used to remove the excess PVP ligands and residual KIT-6 by solvent extraction. The final product was purified by centrifugation, and the precipitated Au NPs were re-dispersed in ethanol or water to form stable colloidal dispersions.

Surface modification of the ordered *meso*-Au NPs with HS-β-CD. In order to promote the interaction between the analytes with low surface affinity and the enhanced Au NPs, a ligand exchange reaction was carried out in the experiment. PVP-capped mesoporous Au NPs were surface modified by mixing 1 ml of 100 ppm HS-β-CD aqueous solution with 2 ml of gold colloids, and then was stirred overnight to complete the chemical modification. To remove the excess HS-β-CD ligands, the resulting mixture was purified by centrifugation at 6000 rpm. The precipitated sample was redispersed in ethanol to form stable colloidal suspensions.

SERS detection of PAHs based on the hydrophobic slippery surface. For PAH detection, the HS-β-CD modified *meso*-Au colloid was used as SERS-active materials, and a hydrophobic slippery surface was used as support substrate. The detailed procedure could be summarized as the following three steps. (i) Interaction between functionalized Au NPs and PAH molecules. 2 mL of anthracene or naphthalene in ethanol were added to 1 mL of HS-β-CD modified mesoporous Au NPs. In order to allow the analytes to fill the cavity of

HS-β-CD, the mixture was stirred for 24 h at room temperature. The resulting Au/PAH sample was centrifuged and redispersed in ethanol. (ii) Preparation of the hydrophobic slippery surface. In brief, 0.5 mL of perfluorinated fluids were coated onto the Teflon membrane by spin coating. The excess lubricating liquids was removed by heating at 80℃, and then the hydrophobic slippery surface was obtained two hours later. (iii) SERS detection. 60 μL of mixed droplet containing analytes and HS-β-CD modified *meso*-Au NPs was dropped onto the hydrophobic slippery surface by using pipette. The heating temperature was 120℃, and the size of droplet reduced gradually during evaporation process. Finally, the sample was dried within 8 min. The diameter of concentrated region was about 0.2 ~ 0.3 mm. Within this tiny spot, the SERS spectra were measured.

Characterization. The morphology of mesoporous Au NPs were characterized using a scanning electron microscope (SEM, JEOL, JSM-7000F) and a transmission electron microscope (TEM, JEOL, JEM-2100 with an accelerating voltage of 200 kV). Bright-field imaging was conducted on a self-made optical testing platform in our laboratory with a mercury lamp as the excited source. SERS detection was conducted on a confocal Raman Spectrometer (LabRAM, HR Evolution). A confocal microscope was used to focus the laser with a 100X objective. The laser wavelength was 633 nm, and the power was about 2 mW. Moreover, the exposure time was 10 s with 2 collection times.

RESULTS AND DISCUSSION

Cyclodextrins are an important class of receptor in supramolecular chemistry, and their cyclic oligosaccharide structures could form hydrophobic internal cavities. With seven glucose units, β-CD has been the most widely used cyclodextrin, and its hydrophobic cavity could provide a model for interaction with molecules to form a host–guest complex by hydrophobic effect.[42] Fig. 1a depicts the proposed strategy for SERS sensing of PAHs with HS-β-CD modified *meso*-Au NPs. The initial PVP-capped gold NPs could be modified with HS-β-CD through a ligand exchange reaction. As a result, the PAHs molecules, with very low affinity to metallic surfaces, could be detected sensitively due to the supramolecular interaction. In addition, a hydrophobic slippery platform is also employed as a concentrator to delivering and enriching the HS-β-CD modified Au/analytes into specific regions, as shown

in Fig 1b. This SERS substrates was simply prepared by depositing a mixed droplet of Au NPs and PAHs molecule on the slippery surface. During solvent evaporation, the droplet volume and contact area decreased gradually due to the low friction of the lubricated Teflon surface. As a result, the diluted Au/analytes can be concentrated into a small area, leading to the aggregated "hot spots" and improved SERS sensitivity.[3]

The monodispersed *meso*-Au NPs, employed as SERS-active materials, are synthesized through a novel "soft-enveloping strategy", which was reported in our previous work.[41] During the chemical synthesis, a 3D mesoporous silica (KIT-6) is employed as a hard template and TMDS is used as the reducing agent. Being insoluble with the gold precursor, hexane solvent is used as a barrier layer to prevent the migrating of metal species to the outside of *meso*-silica channels. TMDS regent could be diffused into the KIT-6 template through the barrier layer, and then react with $HAuCl_4$ at the interfaces of solid-liquid phase. As a result, the ordered Au networks are successfully duplicated within the mesoporous channels of KIT-6 template. Finally, the stable and disperse *meso*-Au NPs modified with PVP ligands was obtained after template removal and surface purification. The SEM image in Fig. 2b shows the shapes of SH-β-CD modified *meso*-Au NPs, indicated that the synthesized Au NPs were isolated from each other and had a narrow particle size distribution. The average diameter of Au networks is about 100 nm, and the morphology is nearly spherical with high uniformity. Due to the features of 3D interior channels with high porosities and surface areas, the colloidal mesoporous Au NPs may show an enhanced absorption behavior towards the detected analytes. Moreover, the morphology of *meso*-Au NPs would provide high-density of "hot spot" regions owing to the interconnected porous configuration, which could be confirmed by the high-magnification TEM image (inset of Fig. 2b).

Due to the low binding ability of PVP ligands to the PAH molecules, a ligand exchange process should be carried out to efficiently capture and concentrate target analytes to the noble metal surface, as shown in Fig. 2a. Here, HS-β-CD molecule was employed to modify the mesoporous nanoparticles via the chemisorption of Au-S covalent bond. Thus, the self-assembled monolayers (SAMs) would be obtained on SERS-active materials prior to target sensing. The formation of SH-β-CD monolayer on the mesoporous Au NPs surface was studied by Raman spectroscopy, as shown in Fig. 2c. The characteristic Raman bands of

SH-β-CD modified Au NPs appeared at 270, 480, 944, 1046 and 1360 cm^{-1}, which agreed well with the vibrational peaks of blank SH-β-CD powder. Moreover, the vibrational peak at 270 cm^{-1} is assigned to the Au-S stretch mode, which indicated that SH-β-CD ligands had been adsorbed on the Au networks successfully.[43] Fig. S1 shows the SERS spectra of *meso*-Au NPs modified with SH-β-CD ranging from 1 ppm to 1000 ppm. The results indicated that the Au networks surface could not be functionalized with capture ligand successfully when the concentration of HS-β-CD was decreased to 1 ppm.

To study the SERS enhancement mechanism of SH-β-CD functionalized *meso*-Au NPs, a controlled experiment was performed. Anthracene, a typical PAHs molecule, was employed as the target analyte, which showed a very low affinity to the PVP-capped gold surfaces (shown in Fig. 3c). In contrast, the hydrophobic anthracene molecule could easily enter the hydrophobic cavity of SH-β-CD to form the inclusion complex (shown in Fig. 3b). As a result, the detected molecule tend to adsorb on the Au NPs surface in the presence of SH-β-CD, and then was efficiently enhanced by the SERS sensor. Typically, the main vibrational peaks of anthracene are located at 750, 1005 and 1482 cm^{-1} (Fig. 3a), which are assigned to C-C out-of-plane stretching combined with C–C–C bending mode, C-H in-plane bending mode, and C–C stretching vibrations, respectively.[40] From Fig. 3a, we can find that it is difficult to detect anthracene directly by using PVP capped mesoporous Au NPs. When the concentration of anthracene was 1 ppm, the results demonstrated very weak Raman signals due to the steric hindrance effect of PVP ligands. However, in the presence of SH-β-CD, the enhanced Raman signals could be clearly observed. The signal amplification phenomenon is mainly due to the host-guest interactions. Consequently, a significant SERS enhancement was obtained by ~50 times, compared to SERS signal enhanced by PVP modified Au networks.

To determine the optimal SH-β-CD surface coverage for PAHs detection, the SERS spectra of *meso*-Au/anthracene complexes is measured, as shown in Fig. 4a. The concentrations of SH-β-CD molecule ranged from 10 ppm to 1000 ppm with a fixed anthracene (1 ppm). Raman spectra of 10 points were collected randomly for each sample and two characteristic bands at 750 and 1005 cm^{-1} were used to get the average Raman intensity. In Fig. 4b, with the increase of SH-β-CD concentration, the SERS intensities of anthracene increase first and then decrease. When the concentration of modified SH-β-CD was 100 ppm,

the maximum intensity of SERS signal appeared. This concentration may corresponds to the optimum number of SH-β-CD ligands covering the mesoporous Au NPs surface. The inset schematic in Fig. 4b demonstrates a possible chemisorption model of HS-β-CD onto mesoporous Au NPs. For 10 ppm of HS-β-CD, the Raman intensity of PAH molecule was low, and a number of anthracene cannot absorb onto the gold surface. With the increase of HS-β-CD concentration, more HS-β-CD captured PAH analytes can locate at the electromagnetic enhanced zone, leading to an improved SERS signal. Then, if the concentration of capture agent increases continuously, e.g., 1000 ppm, it will exceed the largest surface coverage for Au networks. A part of redundant HS-β-CD/anthracene complexes cannot absorb onto the Au surface, and thus the SERS signals cannot be further amplified.[30] Consequently, an optimized concentration of 100 ppm was obtained for the functionalization of mesoporous Au NPs and the subsequent SERS sensing.

It is known that SERS detection is a relatively complicated system, which refers to the interactions among incident laser, plasmonic nanostructures, and target molecule. For a typical metal colloids-based SERS detection, the preparation of SERS substrates is simply depositing a droplet of colloidal metal nanoparticles and target molecule on a support substrate. After the solvent drying, the SERS signals are collected on the substrate. For the given *meso*-Au NPs, the absorption behavior between plasmonic Au NPs and target molecule play a vital role in the SERS detection. Here, the influences of surface ligands of Au networks and support substrates on the SERS enhancement of PAH are investigated, as presented in Fig. 5a. The schematic shows three kinds of detection routes based on various surface ligands modified Au NPs and support substrates: i). PVP modified Au networks supported by silicon wafer (method 1); ii). SH-β-CD modified Au networks supported by silicon wafer (method 2); iii). SH-β-CD modified Au networks supported by hydrophobic slippery surface (method 3). Moreover, an optimized droplet volume was obtained for SERS detection, i.e., 10 μL colloidal mesoporous Au NPs and 50 μL target molecule.

SERS detection supported by silicon wafer is the most common route for Au or Ag colloids. For method 1 and method 2, a typical ‘‘coffee-ring’’ pattern appear after droplet evaporation, as shown in Fig. S2. This phenomenon was mainly ascribed to the pinning effects of contact line and capillary flowing from the center to the margin of droplet. As a

result, the analytes or HS-β-CD modified *meso*-Au NPs diffused freely over silicon wafer during evaporation, leading to the random distribution of molecules and plasmonic Au NPs. Fig. 5c illustrates that the method 3 shows the most sensitive SERS performance. By employing PVP functionalized Au networks as SERS-active materials, the lowest detection concentration of anthracene is 1 ppm, as shown in Fig. 5c and Fig. S3. The bad SERS enhancement may be due to the fact that a proportion of analytes cannot be efficiently excited by the enhanced near-fields. When PVP was replaced by HS-β-CD via a ligand exchange process, the lowest detection concentration could be reduced to 0.01 ppm (Fig. S4), which be mainly ascribed to the effect of host-guest interaction. In addition, if a hydrophobic slippery surface was employed as the support substrate, the droplet containing *meso*-Au NPs and anthracene is condensed into a very limited area, as shown in Fig. S5. Combined this enrichment strategy with the host-guest effect of HS-β-CD ligands, the detection limits of anthracene molecule could be remarkably improved, showing 2–3 orders of higher sensitivity (shown in Figure 5b and 5c). When the concentration of anthracene was 1 ppm, all characteristic peaks could be distinguishable and the occurrence probability was 100%. When the concentration was reduced to 0.01 ppm, the detection probability was reduced to ~78%. Even for the ultra-low 1 ppb, the probability to collect observable SERS signals remained at ~ 40%, showing extremely low SERS detection limit for PAH molecule.

Such high SERS enhancement is mainly attributed to the following aspects: 1). The mesopores nanostructure of Au networks. Due to the feature of large surface area and high-density mesopores, an improved absorption and modification behavior could be obtained for HS-β-CD ligands and target molecules. Besides, the mesoporous Au NPs possess abundant "hot spot" regions owing to the interconnected porous configuration. 2) The host–guest interaction between Au NPs and target molecule. The SERS signals of PAHs could be also improved owing to the cavity structure of functional group, which is capable of adsorbing analytes to form the host (HS-β-CD)–guest (PAHs) complex. Therefore, the anthracene molecule is captured and concentrated near the surface of SERS-enhanced Au NPs, leading to the improved SERS performance. 3) The enrichment effect of hydrophobic slippery surface. Due to the low surface tension of perfluorinated fluids, the "coffee ring" effect could be eliminated during the droplet's evaporation. The diluted HS-β-CD modified Au–PAHs

complex could be enriched to a very limited area, e.g. ~ 0.2 mm in diameter, while the initial size of droplet was ~ 8 mm in diameter. Thus, the aggregated mesoporous Au NPs/analytes can further improve the SERS sensitivity.

To date, due to the heterogeneous distribution of metal nanoparticles on a SERS substrate, in combination with the small size of the focused laser spot, it still remains a challenge to employ SERS as a reliable quantitative technique. The ratiometric method offers an alternative way to achieve sensitive and reproducible SERS detection by offering an internal calibration to correct the signal fluctuation. Here, besides the role of capture ligand for PAHs, HS-β-CD could also be served as a built-in corrections to achieve quantitative SERS detection. The vibrational peak at 480 cm^{-1} was regarded as an internal standard, and the Raman intensities at 750 and 1005 cm^{-1} were employed to evaluate the SERS sensitivity of *meso*-Au NPs, which increased along with the increment of anthracene concentrations (Fig. 5b). It can be clearly seen that the SERS ratios of (I_{750}/I_{480}) and (I_{1005}/I_{480}) shows a good linearity with the negative logarithm of anthracene concentrations, resulting in a ratiometric determination in the range from 1 ppm to 1 ppb (Fig. 5d and 5e). By contrast, an irregular variation is observed through the relationship between the SERS intensities of 750 or 1005 cm^{-1} and the negative logarithm of anthracene (Fig. S6). In addition, the performance of Raman signal uniformity was also evaluated by using HS-β-CD as the internal standard (Fig. S7). For the bands of 750 cm^{-1} and 1005 cm^{-1}, the relative standard deviation (RSD) values were 7.3% and 9.5%, respectively.

Given the sensitive response of HS-β-CD modified *meso*-Au NPs towards PAHs, the SERS sensing of naphthalene is also investigated, as shown in Fig. 6a. As a typical environmental pollutant, naphthalene exists in air, aqueous phases and oils, and has a potential health hazard, e.g., injuring liver and nervous system. The main characteristic Raman peaks are located at 808, 914, 1172, 1378, 1579, and 1610 cm^{-1}, which could be identified even at a concentration of 10 ppb. Fig. 6b shows the linear response of ratiometric SERS intensity (I_{1378}/I_{480}) along with the increment of naphthalene concentrations ranging from 10 ppm to 10 ppb. The sensitive and quantitative detection of various PAH molecules indicates that the HS-β-CD functionalized mesoporous Au NPs combined with hydrophobic slippery surface, could be an effective strategy to realize real-world SERS applications for

PAH molecules.

CONCLUSION

In summary, a novel PAHs detection strategy was developed by using capture ligands modified *meso*-Au NPs as SERS-active materials and hydrophobic slippery surface as support substrate. SH-β-CD molecule was employed to modify the Au networks via the Au-S covalent bond, and then efficiently capture target analytes to the noble metal surface. Compared to the PVP modified Au NPs, a significant enhanced SERS signal for anthracene molecule, e.g., ~50 times, was obtained based on the SH-β-CD functionalized *meso*-Au NPs. We also optimized the surface coverage of capture ligands for sensitive PAHs detection, which was 100 ppm of SH-β-CD. With the aid of a hydrophobic slippery surface, the lowest detection limits of anthracene could be as low as 1ppb, showing excellent SERS sensitivity. Moreover, HS-β-CD could also be served as a built-in corrections, and a good linear correlation between intensity ratios of (I_{750}/I_{480}) and (I_{1005}/I_{480}) and negative logarithm of anthracene concentrations was obtained, may providing a potential application platform for quantitative PAHs monitoring in realistic fields.

ASSOCIATED CONTENT

Supporting Information

The Supporting Information is available free of charge on the ACS Publications website at DOI:

AUTHOR INFORMATION

Corresponding Authors

*E-mail: jxfang@mail.xjtu.edu.cn. Tel: +86-82668150

ACKNOWLEDGMENTS

This work was supported by the programs supported by the National Natural Science Foundation of China (Nos. 21675122 and 21874104), Shaanxi Province Key Industries Innovation Chain Project (2019ZDLSF07-08), the World-Class Universities (Disciplines), the Characteristic Development Guidance Funds for the Central Universities, and the Fundamental Research Funds for the Central Universities. The Raman measurement was supported by Instrument Analysis Center of Xi'an Jiaotong University.

REFERENCES

1. Wang, Y. H.; Wei, J.; Radjenovic, P.; Tian, Z. Q.; Li, J. F. In Situ Analysis of Surface Catalytic Reactions Using Shell-Isolated Nanoparticle-Enhanced Raman Spectroscopy. *Analytical Chemistry* **2019,** *91* (3), 1675-1685.

2. Xu, M.; Ma, X.; Wei, T.; Lu, Z. X.; Ren, B. In Situ Imaging of Live-Cell Extracellular pH during Cell Apoptosis with Surface-Enhanced Raman Spectroscopy. *Analytical Chemistry* **2018,** *90* (23), 13922-13928.

3. Zhang, D.; You, H.; Yuan, L.; Hao, R.; Li, T.; Fang, J. Hydrophobic Slippery Surface-Based Surface-Enhanced Raman Spectroscopy Platform for Ultrasensitive Detection in Food Safety Applications. *Analytical Chemistry* **2019,** *91* (7), 4687-4695.

4. Nguyen, T. D.; Song, M. S.; Ly, N. H.; Lee, S. Y.; Joo, S.-W. Nanostars on Nanopipette Tips: A Raman Probe for Quantifying Oxygen Levels in Hypoxic Single Cells and Tumours. *Angewandte Chemie International Edition* **2019,** *58* (9), 2710-2714.

5. Zrimsek, A. B.; Chiang, N.; Mattei, M.; Zaleski, S.; McAnally, M. O.; Chapman, C. T.; Henry, A.-I.; Schatz, G. C.; Van Duyne, R. P. Single-Molecule Chemistry with Surface- and Tip-Enhanced Raman Spectroscopy. *Chemical Reviews* **2017,** *117* (11), 7583-7613.

6. Tian, L.; Su, M.; Yu, F.; Xu, Y.; Li, X.; Li, L.; Liu, H.; Tan, W. Liquid-state quantitative SERS analyzer on self-ordered metal liquid-like plasmonic arrays. *Nature Communications* **2018,** *9*, 3642.

7. Dong, J. C.; Zhang, X.-G.; Briega-Martos, V.; Jin, X.; Yang, J.; Chen, S.; Yang, Z.-L.; Wu, D.-Y.; Feliu, J. M.; Williams, C. T.; Tian, Z.-Q.; Li, J.-F. In situ Raman spectroscopic evidence for oxygen reduction reaction intermediates at platinum single-crystal surfaces. *Nature Energy* **2019,** *4* (1), 60-67.

8. Nie, S. M.; Emery, S. R. Probing single molecules and single nanoparticles by surface-enhanced Raman scattering. *Science* **1997,** *275* (5303), 1102-1106.

9. Kim, D. S.; Honglawan, A.; Yang, S.; Yoon, D. K. Arrangement and SERS Applications of Nanoparticle Clusters Using Liquid Crystalline Template. *ACS applied materials & interfaces* **2017,** *9* (8), 7787-7792.

10. Li, H.; Yang, Q.; Hou, J.; Li, Y.; Li, M.; Song, Y. Bioinspired Micropatterned

Superhydrophilic Au-Areoles for Surface-Enhanced Raman Scattering (SERS) Trace Detection. *Advanced Functional Materials* **2018,** *28* (21), 1800448.

11. Liu, S.-Y.; Tian, X.-D.; Zhang, Y.; Li, J.-F. Quantitative Surface-Enhanced Raman Spectroscopy through the Interface-Assisted Self-Assembly of Three-Dimensional Silver Nanorod Substrates. *Analytical Chemistry* **2018,** *90* (12), 7275-7282.

12. Zhang, D.; Fang, J.; Li, T. Sensitive and uniform detection using Surface-Enhanced Raman Scattering: Influence of colloidal-droplets evaporation based on Au-Ag alloy nanourchins. *Journal of Colloid and Interface Science* **2018,** *514*, 217-226.

13. Peng, Q.; Wang, N.; Zhu, Y.; Hu, J.; Peng, H.; Li, L.; Zheng, B.; Du, J.; Xiao, D. Hydrophobic AgNPs: one-step synthesis in aqueous solution and their greatly enhanced performance for SERS detection. *Journal of Materials Chemistry C* **2019,** *7* (34), 10465-10470.

14. Park, J.-E.; Lee, Y.; Nam, J.-M. Precisely Shaped, Uniformly Formed Gold Nanocubes with Ultrahigh Reproducibility in Single-Particle Scattering and Surface-Enhanced Raman Scattering. *Nano Letters* **2018,** *18* (10), 6475-6482.

15. Indrasekara, A. S. D. S.; Meyers, S.; Shubeita, S.; Feldman, L. C.; Gustafsson, T.; Fabris, L. Gold nanostar substrates for SERS-based chemical sensing in the femtomolar regime. *Nanoscale* **2014,** *6* (15), 8891-8899.

16. Ding, S.-Y.; You, E.-M.; Tian, Z.-Q.; Moskovits, M. Electromagnetic theories of surface-enhanced Raman spectroscopy. *Chemical Society Reviews* **2017,** *46* (13), 4042-4076.

17. Lee, H. K.; Lee, Y. H.; Koh, C. S. L.; Gia Chuong, P.-Q.; Han, X.; Lay, C. L.; Sim, H. Y. F.; Kao, Y.-C.; An, Q.; Ling, X. Y. Designing surface-enhanced Raman scattering (SERS) platforms beyond hotspot engineering: emerging opportunities in analyte manipulations and hybrid materials. *Chemical Society Reviews* **2019,** *48* (3), 731-756.

18. Chen, H.-Y.; Lin, M.-H.; Wang, C.-Y.; Chang, Y.-M.; Gwo, S. Large-Scale Hot Spot Engineering for Quantitative SERS at the Single-Molecule Scale. *Journal of the American Chemical Society* **2015,** *137* (42), 13698-13705.

19. Szlag, V. M.; Rodriguez, R. S.; He, J.; Hudson-Smith, N.; Kang, H.; Le, N.; Reineke, T. M.; Haynes, C. L. Molecular Affinity Agents for Intrinsic Surface-Enhanced Raman Scattering (SERS) Sensors. *ACS applied materials & interfaces* **2018,** *10* (38), 31825-31844.

20. Tang, S.; Li, Y.; Huang, H.; Li, P.; Guo, Z.; Luo, Q.; Wang, Z.; Chu, P. K.; Li, J.; Yu, X. F. Efficient Enrichment and Self-Assembly of Hybrid Nanoparticles into Removable and Magnetic SERS Substrates for Sensitive Detection of Environmental Pollutants. *ACS applied materials & interfaces* **2017,** *9* (8), 7472-7480.

21. Lu, H.; Zhu, L.; Zhang, C.; Chen, K.; Cui, Y. Mixing Assisted "Hot Spots" Occupying SERS Strategy for Highly Sensitive In Situ Study. *Analytical Chemistry* **2018,** *90* (7), 4535-4543.

22. Zhang, L.; Hao, R.; Zhang, D.; You, H.; Dai, Y.; Liu, W.; Fang, J. Shape-Controlled Hierarchical Flowerlike Au Nanostructure Microarrays by Electrochemical Growth for Surface-Enhanced Raman Spectroscopy Application. *Analytical chemistry* **2020**, *92*(14), 9838-9846.

23. Zhou, B.; Mao, M.; Cao, X.; Ge, M.; Tang, X.; Li, S.; Lin, D.; Yang, L.; Liu, J. Amphiphilic Functionalized Acupuncture Needle as SERS Sensor for In Situ Multiphase Detection. *Analytical Chemistry* **2018,** *90* (6), 3826-3832.

24. Lu, L.-Q.; Zheng, Y.; Qu, W.-G.; Yu, H.-Q.; Xu, A.-W. Hydrophobic Teflon films as concentrators for single-molecule SERS detection. *Journal of Materials Chemistry* **2012,** *22* (39), 20986-20990.

25. Kim, N. H.; Hwang, W.; Baek, K.; Rohman, M. R.; Kim, J.; Kim, H. W.; Mun, J.; Lee, S. Y.; Yun, G.; Murray, J.; Ha, J. W.; Rho, J.; Moskovits, M.; Kim, K. Smart SERS Hot Spots: Single Molecules Can Be Positioned in a Plasmonic Nanojunction Using Host Guest Chemistry. *Journal of the American Chemical Society* **2018,** *140* (13), 4705-4711.

26. Zhang, D.; Peng, L.; Shang, X.; Zheng, W.; You, H.; Xu, T.; Ma, B.; Ren, B.; Fang, J. Buoyant particulate strategy for few-to-single particle-based plasmonic enhanced nanosensors. *Nature Communications* **2020,** *11* (1), 2603.

27. Shin, S.; Lee, J.; Lee, S.; Kim, H.; Seo, J.; Kim, D.; Hong, J.; Lee, S.; Lee, T. A Droplet-Based High-Throughput SERS Platform on a Droplet-Guiding-Track-Engraved Superhydrophobic Substrate. *Small* **2017,** *13* (7), 1602865.

28. Lee, M.; Oh, K.; Choi, H.-K.; Lee, S. G.; Youn, H. J.; Lee, H. L.; Jeong, D. H. Subnanomolar Sensitivity of Filter Paper-Based SERS Sensor for Pesticide Detection by Hydrophobicity Change of Paper Surface. *Acs Sensors* **2018,** *3* (1), 151-159.

29. Yu, Z.; Grasso, M. F.; Sorensen, H. H.; Zhang, P. Ratiometric SERS detection of polycyclic aromatic hydrocarbons assisted by beta-cyclodextrin-modified gold nanoparticles. *Mikrochimica acta* **2019,** *186* (6), 391.

30. Xie, Y.; Wang, X.; Han, X.; Song, W.; Ruan, W.; Liu, J.; Zhao, B.; Ozaki, Y. Selective SERS detection of each polycyclic aromatic hydrocarbon (PAH) in a mixture of five kinds of PAHs. *Journal of Raman Spectroscopy* **2011,** *42* (5), 945-950.

31. Qu, L. L.; Li, Y.-T.; Li, D.-W.; Xue, J.-Q.; Fossey, J. S.; Long, Y.-T. Humic acids-based one-step fabrication of SERS substrates for detection of polycyclic aromatic hydrocarbons. *Analyst* **2013,** *138* (5), 1523-1528.

32. Zhang, M.; Zhang, X.; Qu, B.; Zhan, J. Portable kit for high-throughput analysis of polycyclic aromatic hydrocarbons using surface enhanced Raman scattering after dispersive liquid-liquid microextraction. *Talanta* **2017,** *175*, 495-500.

33. Jiang, M.; Qian, Z.; Zhou, X.; Xin, X.; Wu, J.; Chen, C.; Zhang, G.; Xu, G.; Cheng, Y. CTAB micelles assisted rGO-AgNP hybrids for SERS detection of polycyclic aromatic hydrocarbons. *Physical Chemistry Chemical Physics* **2015,** *17* (33), 21158-21163.

34. Gao, Y.; Li, L.; Zhang, X.; Wang, X.; Ji, W.; Zhao, J.; Ozaki, Y. CTAB-triggered Ag aggregates for reproducible SERS analysis of urinary polycyclic aromatic hydrocarbon metabolites. *Chemical Communications* **2019,** *55* (15), 2146-2149.

35. Jency, D. A.; Umadevi, M.; Sathe, G. V. SERS detection of polychlorinated biphenyls using beta-cyclodextrin functionalized gold nanoparticles on agriculture land soil. *Journal of Raman Spectroscopy* **2015,** *46* (4), 377-383.

36. Zhu, C.; Meng, G.; Huang, Q.; Li, Z.; Huang, Z.; Wang, M.; Yuan, J. Large-scale well-separated Ag nanosheet-assembled micro-hemispheres modified with HS-beta-CD as effective SERS substrates for trace detection of PCBs. *Journal of Materials Chemistry* **2012,** *22* (5), 2271-2278.

37. Olson, L. G.; Uibel, R. H.; Harris, J. M. C18-modified metal-colloid substrates for surface-enhanced Raman detection of trace-level polycyclic aromatic hydrocarbons in aqueous solution. *Applied Spectroscopy* **2004,** *58* (12), 1394-1400.

38. Jia, S.; Li, D.; Fodjo, E. K.; Xu, H.; Deng, W.; Wu, Y.; Wang, Y. Simultaneous preconcentration and ultrasensitive on-site SERS detection of polycyclic aromatic

hydrocarbons in seawater using hexanethiol-modified silver decorated graphene nanomaterials. *Analytical Methods* **2016,** *8* (42), 7587-7596.

39. Xie, Y.; Wang, X.; Han, X.; Xue, X.; Ji, W.; Qi, Z.; Liu, J.; Zhao, B.; Ozaki, Y. Sensing of polycyclic aromatic hydrocarbons with cyclodextrin inclusion complexes on silver nanoparticles by surface-enhanced Raman scattering. *Analyst* **2010,** *135* (6), 1389-1394.

40. Shi, X.; Kwon, Y. H.; Ma, J.; Zheng, R.; Wang, C.; Kronfeldt, H. D. Trace analysis of polycyclic aromatic hydrocarbons using calixarene layered gold colloid film as substrates for surface-enhanced Raman scattering. *Journal of Raman Spectroscopy* **2013,** *44* (1), 41-46.

41. Fang, J.; Zhang, L.; Li, J.; Lu, L.; Ma, C.; Cheng, S.; Li, Z.; Xiong, Q.; You, H. A general soft-enveloping strategy in the templating synthesis of mesoporous metal nanostructures. *Nature Communications* **2018,** *9*, 521.

42. Zhou, Y.; Li, J.; Zhang, L.; Ge, Z.; Wang, X.; Hu, X.; Xu, T.; Li, P.; Xu, W. HS-beta-cyclodextrin-functionalized Ag@Fe3O4@Ag nanoparticles as a surface-enhanced Raman spectroscopy substrate for the sensitive detection of butyl benzyl phthalate. *Analytical and Bioanalytical Chemistry* **2019,** *411* (22), 5691-5701.

43. Bandyopadhyay, S.; Chattopadhyay, S.; Dey, A. The protonation state of thiols in self-assembled monolayers on roughened Ag/Au surfaces and nanoparticles. *Physical Chemistry Chemical Physics* **2015,** *17* (38), 24866-24873.

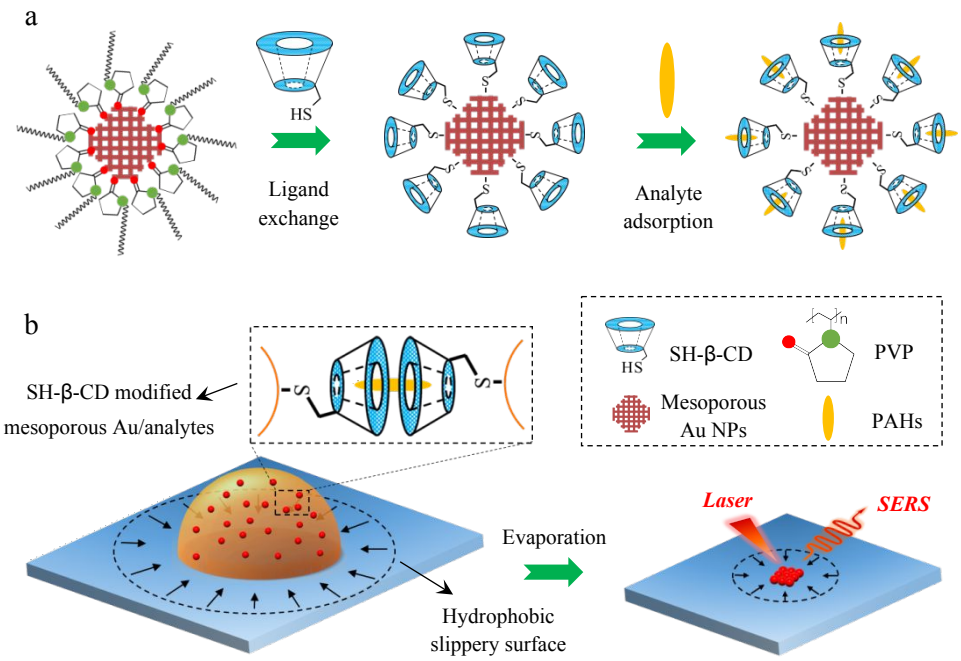

Fig 1. Schematic representation of the effective capture procedure and SERS detection of PAHs molecules based on the ordered *meso*-Au NPs. (a) Surface modification of the Au networks with SH-β-CD ligands to effectively capture the target PAHs molecules. (b) Sensitive SERS detection of PAHs molecules based on the enrichment effect of hydrophobic slippery surface.

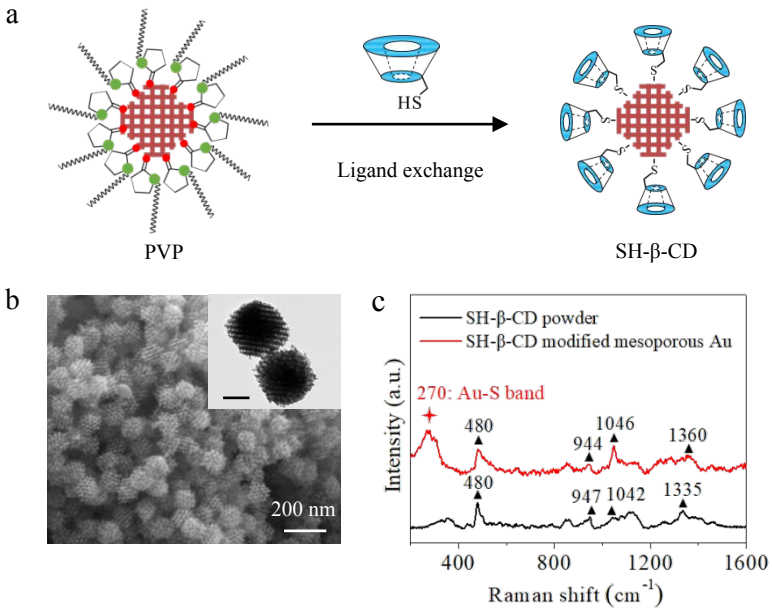

Fig 2. Characterizations of *meso*-Au NPs before and after the modification of SH-β-CD. (a) Schematic illustration of the ligand-exchange between PVP and SH-β-CD. (b) SEM image of SH-β-CD modified *meso*-Au NPs. Inset shows the TEM image with higher magnification. The scale bar was 50 nm. (c) Raman spectrum of *meso*-Au NP capped with SH-β-CD ligand.

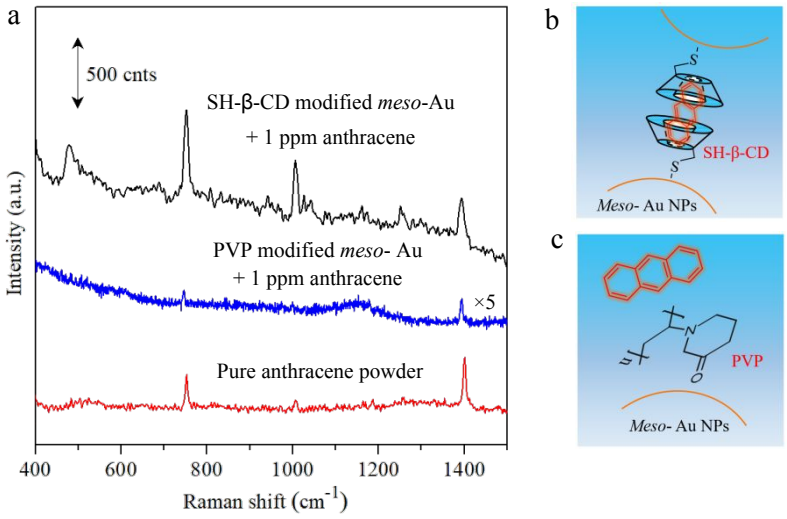

Fig 3. The enhancement principle for SERS detection of probe molecule with weak surface affinity. (a) Raman spectrum of anthracene enhanced by *meso*-Au NPs capped with different ligands. The schematics of obsorption behavior between analytes and Au networks functionlized with (b) SH-β-CD and (c) PVP ligands.

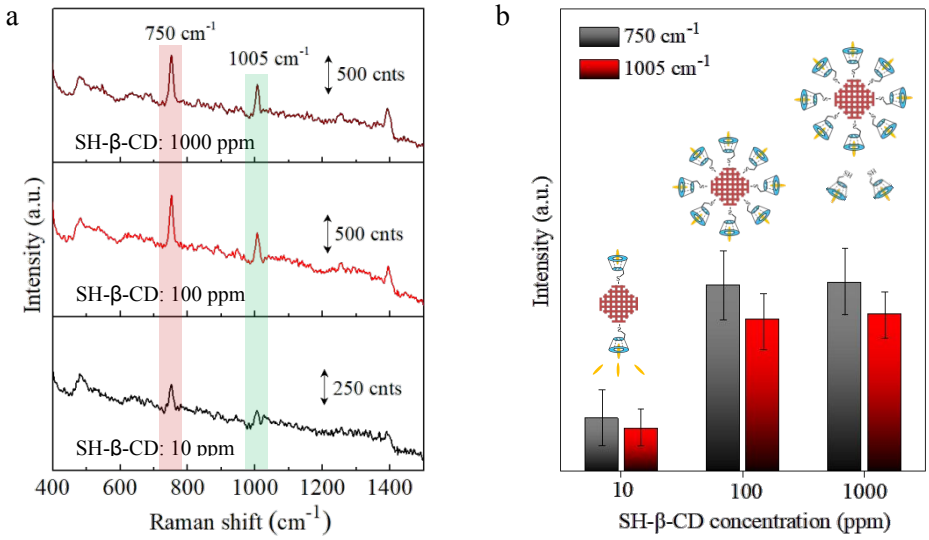

Fig 4. Influence of SH-β-CD concentration on the SERS enhancement of anthracene. (a) SERS spectra of anthracene while the concentrations of SH-β-CD ranging from 10 ppm to 1000 ppm. (b) The compared averaged Raman intensities of anthracene at 750 and 1005 cm^{-1} bands. Insets show the scheme of Au networks with different SH-β-CD surface coverages.

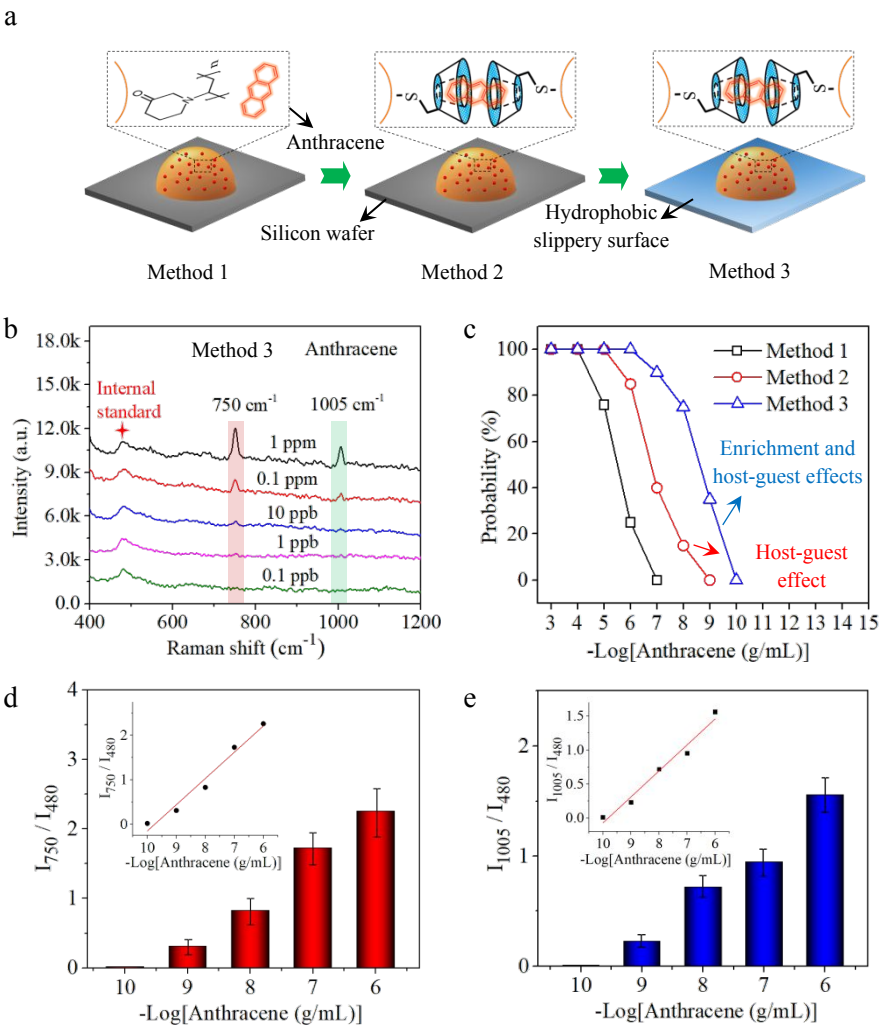

Fig 5. The SERS properties of SH-β-CD modified *meso*-Au NPs. (a) The schematic of SERS mesearements based on the mesoporous Au NPs with various surface ligands and support substrates: i). PVP modified Au networks supported by silicon wafer (method 1); ii). SH-β-CD modified Au networks supported by silicon wafer (method 2); iii). SH-β-CD modified Au networks supported by hydrophobic slippery surface (method 3). (b) SERS spectra of anthracene molecule ranging from 1 ppm to 0.1 ppb with method 3. (c) The detection probability of SERS signals for three types of SERS detection methods. The ratiometric SERS intensities of (d) I_{750}/I_{480} and (e) I_{1005}/I_{480} versus anthracene concentration. Insets show the linear plots for anthracene based on the SH-β-CD modified *meso*-Au NPs.

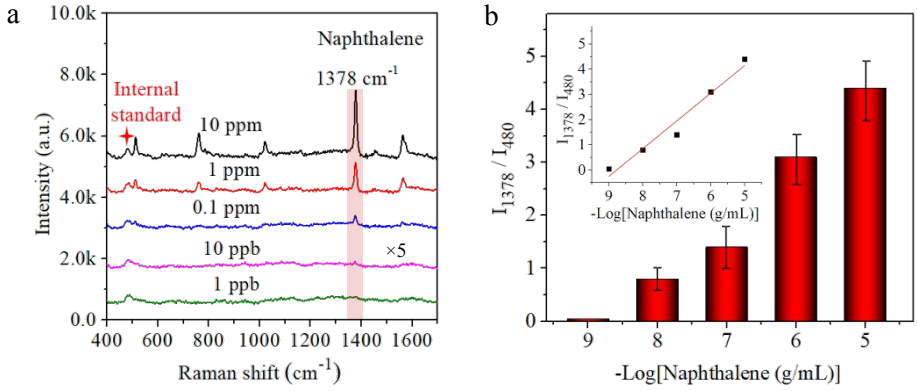

Fig 6. The SERS detection of naphthalene molecule based on SH-β-CD modified *meso*-Au NPs. (a) SERS spectra of naphthalene with different concentrations ragaing from 10 ppm to 1 ppb. (b) The ratiometric SERS intensities of I_{1378}/I_{480} versus naphthalene concentration. Insets show the linear plots for naphthalene based on the SH-β-CD modified *meso*-Au NPs.

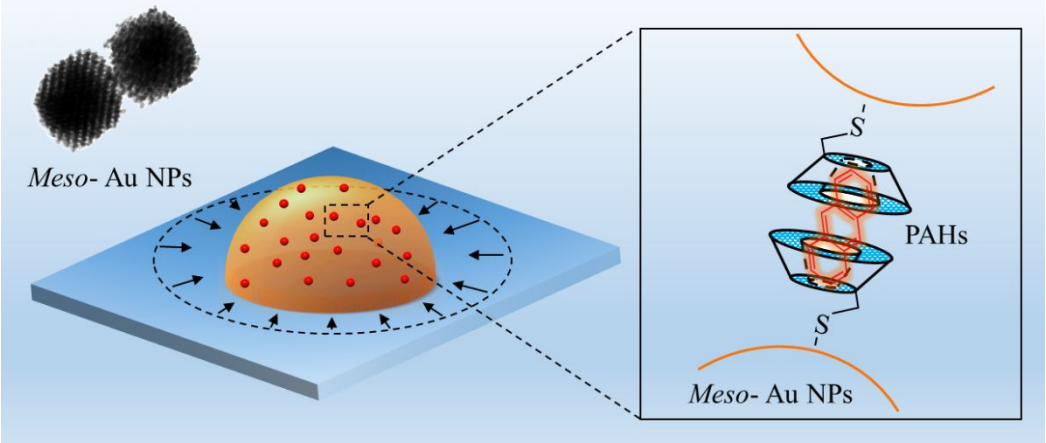

Table of Contents Graphic